Temperature dependence of the dielectric function and the interband critical points in orthorhombic GeS

S. Logothetidis,* P. Lautenschlager, and M. Cardona
Max-Planck-Institut für Festkörperforschung, Heisenbergstrasse 1, D-7000 Stuttgart 80, Federal Republic of Germany
(Received 13 August 1985)

The dielectric function of orthorhombic GeS has been measured ellipsometrically in the 1.66–5.6-eV photon-energy region as a function of temperature between 84 and 500 K. The second derivatives with respect to frequency of the real and imaginary parts of the dielectric function, obtained numerically from the measured spectra with the electric field vector $\mathscr{E}$ parallel to the **a** and **b** axes, show distinct interband critical points that are rather different for the two polarizations. The line shapes of these structures have been fitted with standard analytic expressions for various types of critical points. The temperature dependence of the critical-point parameters obtained for the two principal polarizations is compared and analyzed in terms of average frequencies of phonons participating in the corresponding electron-phonon interaction.

I. INTRODUCTION

In a recent paper[1] we used automatic-rotating-analyzer ellipsometry to study the dielectric tensor of biaxial crystals. As a model we chose the orthorhombic IV-VI compounds (GeS-GeSe-SnS-SnSe). In this paper we show that rotating-analyzer ellipsometry can be used to investigate the temperature dependence of the various components of the dielectric function and its associated critical points in a biaxial crystal. We illustrate this with the example of GeS. We present data for the components of the dielectric tensor of GeS along the **a** and **b** axes at temperatures between 84 and 500 K. The data exhibit a number of structures which were enhanced, as usual,[2,3] by numerically taking the second derivative with respect to photon energy and fitting the structure around critical points (CP's) with standard analytic expressions for their line shapes. We find that all critical-point energies (E) decrease with increasing temperature in a way similar to that found in most semiconductors [note, however, that for the related compounds PbS, PbSe, and PbTe the lowest gap increases with increasing T (Refs. 4 and 5)]. The Lorentzian width (Γ) also increases with increasing T, as expected for decay of the electronic state into the electronic continuum through absorption and emission of phonons. From the fits with standard line shapes we also obtain the critical-point strengths (A) and the excitonic phase shifts (Φ). The former turn out to be nearly independent of temperature for light polarized parallel to the **b** direction ($\mathscr{E}||\mathbf{b}$) and temperature dependent for most structures for $\mathscr{E}||\mathbf{a}$, while the excitonic phase in many cases decreases with increasing temperature, as in other semiconductors.[2,3] The low-temperature spectra show considerable sharpening of some peaks, especially for $\mathscr{E}||\mathbf{a}$.

II. EXPERIMENTAL DETAILS

Undoped single crystals of GeS were grown by vacuum sublimation.[6] Ellipsometric measurements on cleaved surfaces were performed for samples that had been oriented using standard Laue x-ray backscattering and accurately cut as 1×1 cm rectangular plates, the sides being the desired crystallographic **a** and **b** axes. All of the samples used showed mirrorlike surfaces with no visible steps. The surface layer was peeled off with adhesive tape immediately before the measurements. When measurements were performed with a different sample orientation with respect to the plane of incidence, the cryostat was opened, the sample rotated, and a new surface was peeled off on the cold finger of the cryostat at room temperature. We closed the cryostat in a N_2 atmosphere and pumped it down to a vacuum better than 2×10^{-8} Torr before cooling. In this way we used freshly cleaved surfaces with a minimum of contamination[7] and we avoided the condensation of ice and other films on the sample, which can be particularly insidious at low temperatures.[8]

III. RESULTS

In a recent paper[1] we obtained the dielectric function of orthorhombic GeS for all three polarizations by means of the multiple-angle-of-incidence (MAI) method[9] from measurements that had been carried out on three different planes of incidence, each containing two principle axes. The two components of the dielectric tensor that correspond to polarizations parallel to the cleavage plane (**a**,**b**) are seen to agree basically with those obtained with an approximate procedure suggested by Aspnes.[10,11] This procedure, which uses only measurements on the easy-cleavage plane at large angles of incidence, is particularly suitable for measurements at several temperatures: The preparation of a reflecting plane perpendicular to the cleavage plane is very delicate and laborious, especially if it has to be repeated several times. Also, inside a cryostat it is hard to vary the angle of incidence, and thus the MAI method becomes impractical. Following the prescription given by Aspnes, we attribute the dielectric function obtained with **a** in the plane of incidence using the ellipsometry program for isotropic materials to the component of the dielectric function for $\mathscr{E}||\mathbf{a}$. Likewise,

for **b** in the plane of incidence we obtained the component for $\mathscr{E}||\mathbf{b}$. This prescription should be accurate for large angles of incidence ϕ. It should be a reasonably good approximation in our case ($\phi=67.5°$), as shown in Fig. 2 of Ref. 1. Thus, we investigate in this work the temperature dependence of the diagonal components of the dielectric function parallel to the **a** and **b** axes of GeS from measurements only on the cleavage plane at 67.5° angle of incidence using the procedure of Ref. 10.

The real and imaginary parts of the components of the dielectric functions for $\mathscr{E}||\mathbf{a}$ and $\mathscr{E}||\mathbf{b}$ ($\varepsilon_a,\varepsilon_b$) measured between 1.66 and 5.6 eV for three selected temperatures are shown in Figs. 1 and 2, respectively. A 20-meV photon-energy mesh was used in all cases. The main feature in these figures is the shift of the whole spectrum to lower energies and its broadening with increasing temperature. We can distinguish in these spectra two regions, one up to ~3.3 eV and another one at higher energies, a behavior similar to that found for the cubic IV-VI materials.[12] We have used the same label[1] for structures in the two principal polarizations that lie very close. The structure labeled E_1' for $\mathscr{E}||\mathbf{a}$ has not been reported before. It appears at low temperatures only for this polarization.

To analyze the structure and obtain the CP parameters, we calculated numerically in the usual manner[2,3] the second-derivative spectra ($d^2\epsilon/d\omega^2$) of the complex dielectric function and fitted them with standard analytic expressions for the two-dimensional (2D) and three-dimensional (3D) CP line shapes:[13,14]

$$\epsilon\sim C-A\ln(E-\omega-i\Gamma)e^{i\Phi}\ \text{(2D)}\,, \tag{1a}$$

$$\epsilon\sim C-A(\omega-E+i\Gamma)^{1/2}e^{i\Phi}\ \text{(3D)}\,. \tag{1b}$$

Values of Φ which are integer multiples of $\pi/2$ correspond to one-electron critical points, while noninteger multiples represent the inclusion of exciton effects.[13,14] In Eq. (1a), taking $A>0$, $\Phi=0$ and $\Phi=\pi/2$ correspond to a minimum and a saddle point, respectively, while in Eq. (1b), $\Phi=0$, $\pi/2$, π, and $3\pi/2$ correspond to M_1, M_2, M_3, and M_0 critical points, respectively.

Figure 3 shows the second-derivative spectra computed from our experimentally obtained real part of the complex

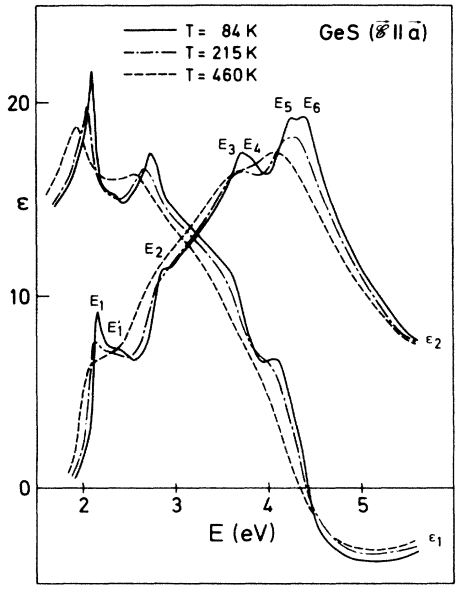

FIG. 1. Real (ϵ_1) and imaginary (ϵ_2) parts of the dielectric function of GeS for light polarized with $\mathscr{E}$ parallel to the **a** axis at 84 K (solid line), 215 K (dashed-dotted line), and 460 K (dashed line).

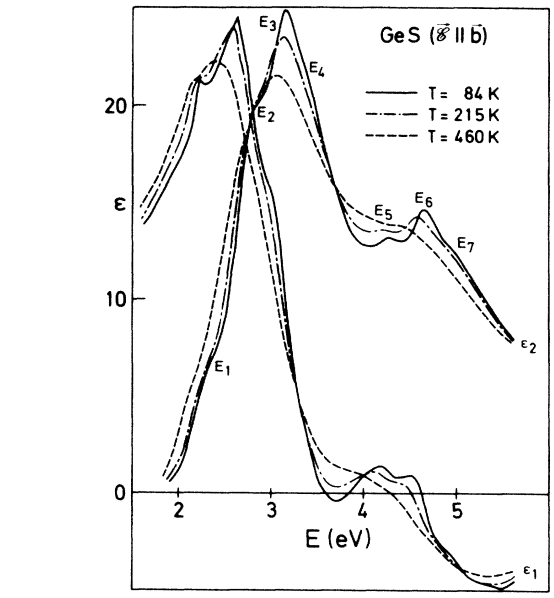

FIG. 2. Real and imaginary parts of the dielectric function of GeS for $\mathscr{E}||\mathbf{b}$. The symbols are the same as in Fig. 1.

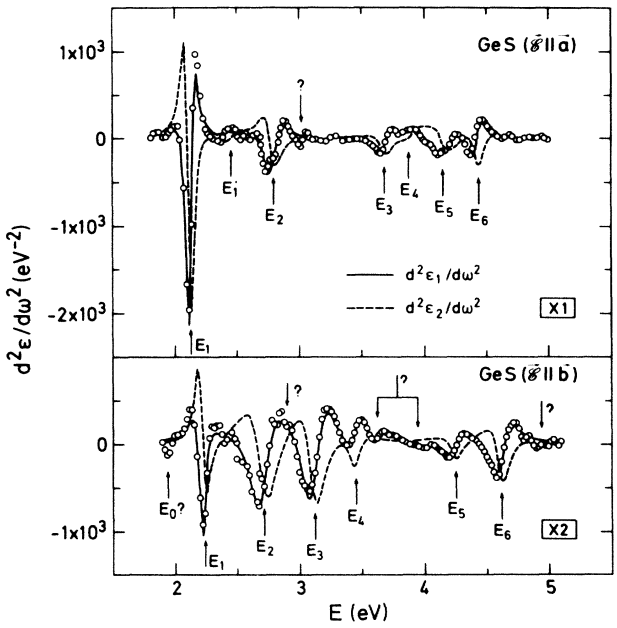

FIG. 3. Fits to the second derivatives of the real (solid line) and imaginary (dashed line) parts of the dielectric function of GeS as a function of energy at 84 K, for the two polarizations studied. The experimental data are only given for $d^3\epsilon_1/d\omega^2$. The vertical scale for $\mathscr{E}||\mathbf{b}$ has been expanded by a factor of 2. The question marks indicate the presence of dubious structures.

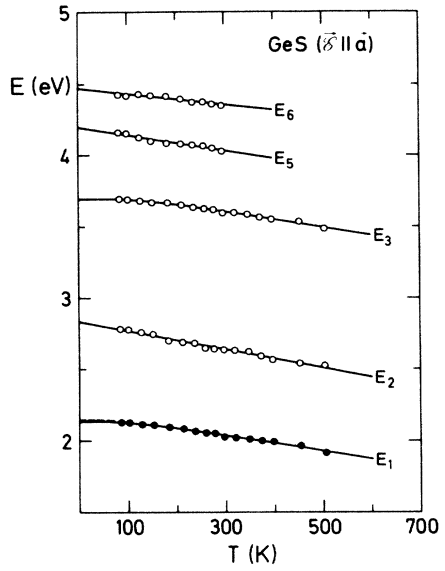

FIG. 4. Temperature dependence of the measured critical-point energies of GeS for $\mathscr{E}||\mathbf{a}$: The dashed line for the E_1 structure corresponds to the fit with Eq. (2b), while the solid lines for all structures represent either fits with Eq. (2a) or linear fits. Typical error bars for the experimental points are given in Table III.

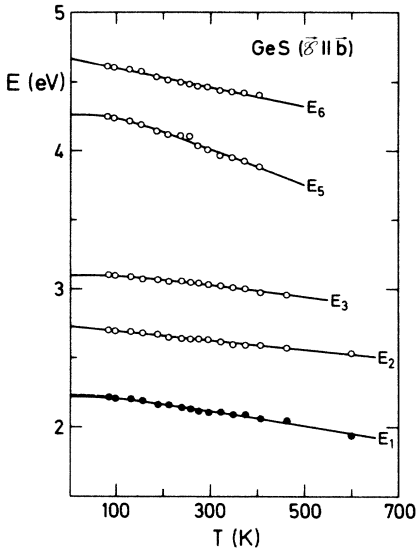

FIG. 5. Same as in Fig. 4, but for $\mathscr{E}||\mathbf{b}$.

dielectric function $d^2\epsilon_1/d\omega^2$ at 84 K for $\mathscr{E}||\mathbf{a}$ and $\mathscr{E}||\mathbf{b}$, together with the best fits using Eqs. (1a) and (1b). This figure reveals considerable structure which is difficult to detect in the primitive spectrum, especially in the $\mathscr{E}||\mathbf{b}$ case (Fig. 2). We also show in this figure the fits to $d^2\epsilon_2/d\omega^2$.

In Figs. 4 and 5 the critical-point energies obtained from our fit to the main transitions for $\mathscr{E}||\mathbf{a}$ and $\mathscr{E}||\mathbf{b}$ in GeS are shown as a function of temperature. The temperature dependences displayed in Figs. 4 and 5 were analyzed with different models: Varshni's relation,[15] a semiempirical relation including a Bose-Einstein statistical factor which takes into account electron-phonon interaction with phonons of an average frequency θ,[2] and a linear dependence on T. We have

TABLE I. Values of the parameters $E(0)$, α, and β obtained by fitting the critical-point energies versus temperature with Eq. (2a). Also, values of E_B, a_B, and θ obtained by fitting with Eq. (2b) and values of E_L and γ obtained by fitting with Eq. (2c) for GeS for the two principle directions parallel to the **a** and **b** axes. The 95% confidence limits are given in parentheses.

	$E(0)$ (eV)	a (10^{-4} eV K^{-1})	β (K)	E_B (eV)	a_B (meV)	θ (K)	E_L (eV)	γ (10^{-4} eV K^{-1})	Type of CP
					$\mathscr{E}||\mathbf{a}$ polarization				
E_1	2.144(15)	6.44(80)	232(120)	2.224(40)	92(50)	317(150)	2.18(1)	4.97(30)	2D minimum and saddle point
E_2							2.832(15)	6.49(50)	2D minimum
E_3	3.708(13)	7.27(90)	351(180)	3.81(5)	113(50)	377(140)	3.75(1)	4.85(40)	M_1 and M_2
E_5							4.12(2)[a]	5.5(8)[a]	2D minimum
E_6							4.45(2)[a]	3.8(8)[a]	2D minimum and saddle point
					$\mathscr{E}||\mathbf{b}$ polarization				
E_1	2.232(24)	5.89(90)	153(130)	2.289(40)	66(40)	239(130)	2.265(12)	5.1(4)	2D minimum
E_2							2.73(1)	3.45(20)	2D minimum and saddle point
E_3	3.109(11)	6.7(2.3)	486(250)	3.186(50)	83(40)	358(120)	3.14(10)	3.8(3)	2D minimum and saddle point
E_5	4.29(4)[b]	15.54(80)	220(160)	4.47(10)	208(100)	300(110)	4.37(20)	11.7(8)	2D minimum
E_6							4.67(10)[b]	7.0(5)	2D minimum and saddle point

[a]Between 84 and 300 K.
[b]Between 84 and 400 K.

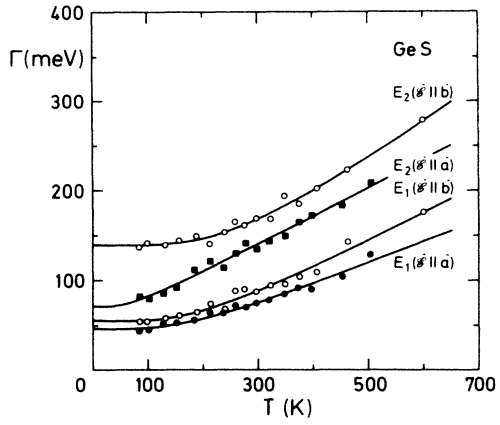

FIG. 6. Temperature dependence of the broadening parameters of the CP's of GeS. The solid lines represent the best fits with an expression proportional to Eq. (2b). Typical error bars for experimental points are given in Table IV.

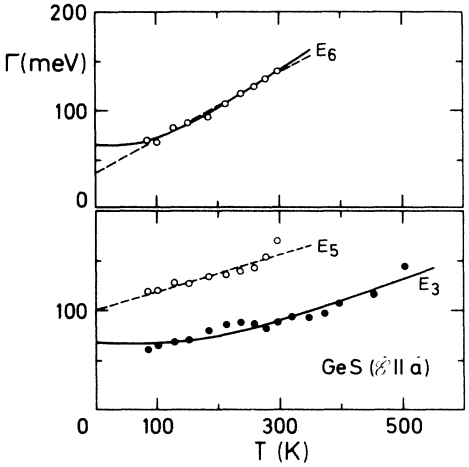

FIG. 7. Temperature dependence of the broadening parameters of the CP's of GeS for $\mathcal{E}||\mathbf{a}$. The solid lines represent the best fits with an expression proportional to Eq. (2b), while the dashed lines give a linear fit. Typical error bars for experimental points are given in Table IV.

$$E(T)=E(0)-\alpha T^2/(T+\beta) \quad \text{(Varshni)}, \tag{2a}$$

$$E(T)=E_B-a_B\left[1+\frac{2}{e^{\theta/T}-1}\right] \quad \text{(Bose-Einstein)}, \tag{2b}$$

$$E(T)=E_L-\gamma T\ . \tag{2c}$$

In Table I we have listed the fit parameters of these models for the two principal components parallel to the **a** and **b** axes. The Lorentzian broadening parameters Γ for the main CP's in the two principal polarizations are displayed in Figs. 6–8 as a function of temperature. The models used for the fits of Figs. 6–8 correspond to an expression proportional to Eq. (2b),[2] and also to a linear dependence on T [Eq. (2c)]. All the coefficients from these fits are represented in Table II. In Fig. 9 we show the temperature dependence of the phase angle Φ, representing the mixture of contiguous CP's for different transitions for polarization $\mathcal{E}||\mathbf{a}$ and for the E_6 structure for $\mathcal{E}||\mathbf{b}$. Finally, in Fig. 10 the strengths of the E_1 structures for the two polarizations, together with those of other structures, are shown as a function of temperature.

IV. DISCUSSION

The two sets of measurements with field orientations along **a** or **b** in the plane of incidence yield approximately the corresponding two principal values of the dielectric

TABLE II. Parameters involved in the temperature dependence of the Lorentzian broadening of the critical points observed in the dielectric function of GeS. The Lorentzian broadening is represented by either $\Gamma(T)=\Gamma_1+\Gamma_0[1+2/(e^{\theta/T}-1)]$ or the linear expression $\Gamma(T)=\Gamma_L+\gamma T$. The 95% confidence limits are given in parentheses.

	Γ_1 (meV)	Γ_0 (meV)	θ (K)	Γ_L (meV)	γ (10^{-4} eV K^{-1})
			$\mathcal{E}||\mathbf{a}$ polarization		
$\Gamma(E_1)$	−16(10)	63(20)	499(150)	25(5)	1.8(2)
$\Gamma(E_2)$	42(20)	29(20)	184(150)	51(7)	3.0(2)
$\Gamma(E_3)$	−10(10)	78(40)	617(300)	47(8)	1.6(3)
$\Gamma(E_5)$				100(16)[a]	1.9(8)[a]
$\Gamma(E_6)$	0(10)	65(30)	295(140)	36(7)[a]	3.4(3)[a]
			$\mathcal{E}||\mathbf{b}$ polarization		
$\Gamma(E_1)$	−39(20)	94(30)	567(190)	24(6)	2.3(3)
$\Gamma(E_2)$	−47(30)	187(50)	785(180)	100(30)	2.6(5)
$\Gamma(E_3)$	−11(10)	124(50)	368(150)	57(10)	5.4(5)
$\Gamma(E_5)$	42(30)	37(30)	152(140)[b]	52(14)	4.7(5)[b]
$\Gamma(E_6)$	58(20)	34(20)	259(160)[b]	73(5)	2.3(2)[b]

[a]Between 84 and 300 K.
[b]Between 84 and 400 K.

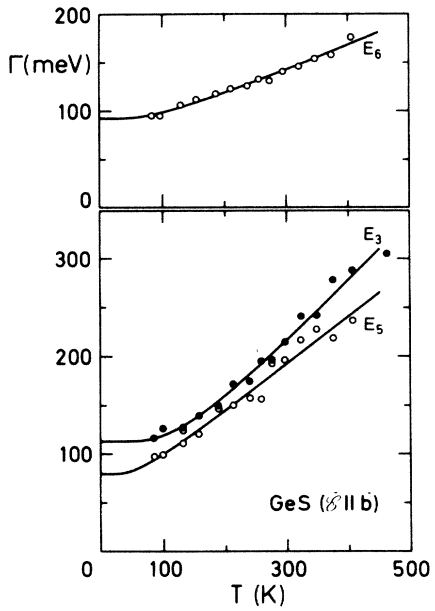

FIG. 8. Temperature dependence of the broadening parameters of the CP's of GeS for $\mathscr{E}||\mathbf{b}$. The solid lines have the same meaning as in Fig. 7.

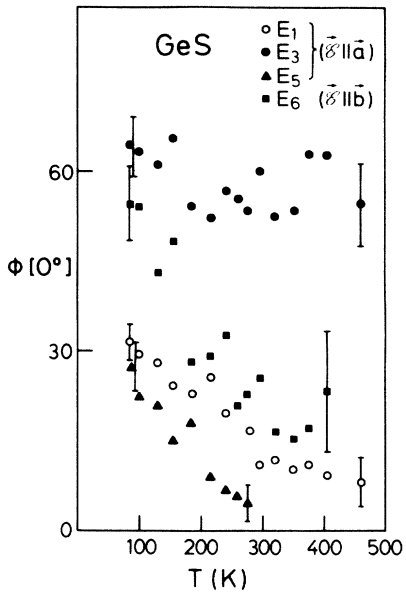

FIG. 9. Temperature dependence of the phase angle Φ defined in Eqs. (1) for the E_1 (open circles), E_3 (solid circles), and E_5 (triangles) CP's for $\mathscr{E}||\mathbf{a}$ and for the E_6 (squares) CP for $\mathscr{E}||\mathbf{b}$.

function. This approximation is extremely good for an angle of incidence $\phi \approx 82°$ (see Fig. 2 of Ref. 1). It introduces errors which are small for $\hbar\omega < 4$ eV, but can reach values $\Delta\epsilon \sim 1.5$ above this photon energy (Fig. 2 of Ref. 1). These errors should not affect significantly the analysis of the derivative spectra and, in particular, their temperature dependence. A glance at Fig. 3 suggests, however, that the structure labeled ? for $\mathscr{E}||\mathbf{a}$ may be "leaking" from the E_3 peak for $\mathscr{E}||\mathbf{b}$. Similar "leakages" (possibly also from the third component of ϵ not measured here) could apply to the peaks labeled ? in Fig. 3 for $\mathscr{E}||\mathbf{b}$.

Some error and "leakage" can also result from a misorientation of the **a** and **b** axes inside of the cryostat. This misorientation should be less than 3° and hence we believe that the corresponding error should be negligible compared to that due to the small angle of incidence ($\phi \approx 67°$ corresponds to an error in the angle required by the expressions used of $\approx 23°$).

An attempt to interpret the critical points observed at room temperature in terms of the band structure of GeS was made in Ref. 1. The discussion there should remain largely valid at all temperatures used in the present measurements since the main effect of the temperature change is to slightly shift and broaden the critical energies and to reduce exciton effects with increasing temperature. We shall not discuss the band-structure assignments any further, especially since they must remain preliminary until calculations of the dielectric function from the electronic band structure become available. Such calculations are underway.[16]

The dimensionality of the critical points resulting from the fits to the present data, and other CP parameters, differ, in some cases, from that given in Ref. 1. The reason lies in the fact that in Ref. 1 only data at room temperature were fitted, while here we have fitted data at all experimental temperatures for a given structure with a critical point of the same dimensionality. At low temperatures the critical points become sharper and it is possible to discriminate better between two and three dimensions. Also, at higher temperature neighboring structures broaden and become indistinguishable. In these cases we have fitted them simultaneously (e.g., $E_5 - E_6$ for $\mathscr{E}||\mathbf{a}$ and $\mathscr{E}||\mathbf{b}$; $E_2 - E_3 - E_4$ for $\mathscr{E}||\mathbf{b}$). This also leads to slightly different parameters than those of Ref. 1.

In Table III we compare the CP energies obtained in

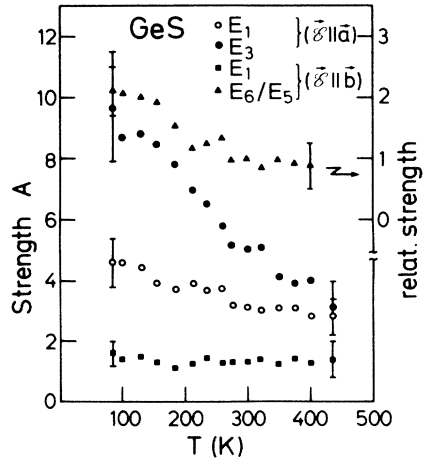

FIG. 10. Temperature dependence of the strength A, defined in Eqs. (1), for the E_1 (open circles) and E_3 (solid circles) structures for $\mathscr{E}||\mathbf{a}$, and E_1 (squares) for $\mathscr{E}||\mathbf{b}$. The right-hand scale corresponds to the ratio of the E_6 and E_5 ($\mathscr{E}||\mathbf{b}$) structures.

TABLE III. Critical-point energies of interband transitions in GeS observed with $\mathscr{E}$ parallel to the **a** and **b** axes at low temperatures, as compared with the results of Ref. 17. All the energies are in eV. The 95% confidence limits are given in parentheses.

	$\mathscr{E}\|\|$**a** polarization			$\mathscr{E}\|\|$**b** polarization	
	Our data 84 K	Ref. 17 100 K		Our data 84 K	Ref. 17 100 K
E_1	2.127(3)	2.115(1)	E_1	2.216(6)	2.21
E_1'	2.43(2)				
E_2	2.78(1)	2.772(5)	E_2	2.67(2)	2.63
				~2.83	2.79
	~3.05				
			E_3	3.10(19)	3.06
E_3	3.695(8)	3.64	E_4	3.44(2)	3.40
				~3.62	3.60
E_4	3.93(2)			~4.0	
E_5	4.16(2)	4.20	E_5	4.251(16)	4.25
E_6	4.44(1)	4.42	E_6	4.614(7)	4.65
			E_7	~4.96	5.0

our work at 84 K for $\mathscr{E}\|\|$**a** and $\mathscr{E}\|\|$**b** to those listed in Ref. 17 obtained at 100 K. With the exception of the E_1' structure for $\mathscr{E}\|\|$**a**, which was not observed in Ref. 17 and may be due to polarization "leakage," the agreement between both sets of data is rather good.

While expressions (2a) and (2c) for the temperature dependence of the critical energies are to be regarded as purely phenomenological, Eq. (2b) corresponds to the microscopic theory of the energy shift induced by electron-phonon interaction.[18] In this theory one must distinguish two contributions: (a) the so-called Debye-Waller terms, which arise from the second-order electron-phonon interaction taken in first-order perturbation theory, and (b) the "Fan" terms, which arise from the first-order interaction in second-order perturbation theory. The "Fan" terms contribute not only an energy shift (real part of self-energy) but also a broadening (imaginary part of self-energy), while Debye-Waller terms yield only an energy shift. Each of the phonons involved contributes to these effects a term $\sim 2n_B+1$, where n_B is the Bose-Einstein occupation number of the phonons. In this manner, Eq. (2b) arises provided one interprets θ as an "average" phonon frequency, appropriately weighted by the electron-phonon coupling constants which tend to increase with increasing phonon frequency[18] and thus weight optical phonons more heavily than acoustic ones. A high-temperature expansion of n_B leads to a linear dependence on T [Eq. (2c)]. This high-temperature dependence is in agreement with Figs. 4 and 5. Several of the variations of critical points with T shown in these figures indicate the decrease in slope required by Eq. (2b) at low temperatures, although the lowest temperature of our measurements (84 K), is not sufficiently low to determine precisely this nonlinear behavior. This is reflected by the large error limits θ and β given in Table I. In fact, in several cases (E_2, E_5, and E_6 for $\mathscr{E}\|\|$**a**; E_2 and E_6 for $\mathscr{E}\|\|$**b**) the data could be best fitted by a linear expression [Eq. (2c)]. In the other cases values of θ between 240 and 380 K were obtained. These values should be compared with the temperatures which correspond to the phonon frequencies of GeS,[19] which have a maximum at ~ 290 cm^{-1} (=430 K). Thus the values of θ found here (240–380 K) are compatible with an average phonon frequency possibly weighted towards the upper frequencies for the reasons discussed above.

Most of the coefficients γ of the linear terms in T given in Table I lie between 3.4×10^{-4} and 7×10^{-4} eV K^{-1}, values which are very similar to those found for interband critical points in other semiconductors.[2,3,20] The energy of the E_5 structure for $\mathscr{E}\|\|$**b**, however, has an exceptionally large coefficient ($\sim 12\times10^{-4}$ eV K^{-1}). This may be a spurious effect resulting from the complex nature of this structure, unresolved at higher temperatures as it includes part of the structure labeled by a question mark in Fig. 3.

The fitted Lorentzian broadening parameters Γ at 84 K, together with their 95% confidence limits, are given in Table IV. They are found to increase with increasing temperaure (Figs. 4–6). Hence they must contain an imaginary self-energy related to the "Fan" terms of the electron-phonon interaction. The measured slope of $\Gamma(T)$ also decreases in most cases with decreasing temperature, a fact which enables us to fit the data with an expression similar to Eq. (2b):

$$\Gamma(T)+\Gamma_1=\Gamma_0\left[1+\frac{2}{e^{\theta/T}-1}\right]. \tag{3}$$

The nonlinearity, however, is also rather small here [nonexistent for $\Gamma(E_5)$ with $\mathscr{E}\|\|$**a**], so that θ can be only determined with poor confidence. Within this confidence the values of θ agree with those found for the critical energies (Table I), although this agreement need not be exact: The phonons which produce the broadening connect electronic states of nearly the same energy (real transitions), while those which produce the shift connect all energies (virtual transitions). Hence the phonons which contribute to the average θ may be different for the real and for the imaginary part of the self-energy. Our data, however, do not allow us, within their large confidence limits, to decide whether such a difference exists. We should point out that for the related material PbS (rocksalt structure) a detailed study of the broadening of critical points

TABLE IV. Broadening parameters of interband transitions in GeS, all in meV at 84 K. The 95% confidence limits are given in parentheses.

$\mathscr{E}\|\|\mathbf{a}$ polarization		$\mathscr{E}\|\|\mathbf{b}$ polarization	
$\Gamma(E_1)$	44(3)	$\Gamma(E_1)$	54(9)
$\Gamma(E_1')$	90(30)		
$\Gamma(E_2)$	82(10)	$\Gamma(E_2)$	137(20)
$\Gamma(E_3)$	61(9)	$\Gamma(E_3)$	116(19)
$\Gamma(E_4)$	94(17)	$\Gamma(E_4)$	110(10)
$\Gamma(E_5)$	119(17)	$\Gamma(E_5)$	97(16)
$\Gamma(E_6)$	83(12)	$\Gamma(E_6)$	95(7)

in the valence band, as obtained from photoemission spectra, has been performed.[21] The observed broadenings increase nearly linearly with temperature with coefficients which lie between 1.4×10^{-4} and 5×10^{-4} eV/K, rather close to those which appear in Table II of this work.

The E_1 structure observed for $\mathscr{E}\|\|\mathbf{a}$ (Fig. 1) at low temperatures shows a steep rise on the low-frequency side which is of the type usually attributed to excitonic effects.[22] This rise becomes less steep as the temperature increases. Also, for reasons not clear to the present authors, the steep rise is not present for $\mathscr{E}\|\|\mathbf{b}$. Note that a sharp edge exciton also appears at ~1.7 eV for $\mathscr{E}\|\|\mathbf{a}$ but not for $\mathscr{E}\|\|\mathbf{b}$.[23,24]

It has become customary[2,3,13,14] to represent excitonic effects with the phase angle Φ of Eqs. (1). This angle is shown in Fig. 9 versus temperature for several of the structures observed. Note that, with the possible exception of E_3, it decreases with increasing T, thus signaling a decrease in excitonic effects with temperature. While this is to be expected on the basis of past experience with similar data, we note that there is, at present, no theory to describe this effect.

In Fig. 10 we have plotted the strengths A obtained from the CP fits [Eqs. (1a) and (1b)] versus T. Note that while the strength of E_1 decreases sharply with T for $\mathscr{E}\|\|\mathbf{a}$, it does not for $\mathscr{E}\|\|\mathbf{b}$, a fact which may be related to the absence of excitonic effects in the latter case. For all other critical points where A is shown in Fig. 10, A decreases slightly with increasing T.

V. CONCLUSIONS

We have shown that spectroscopic ellipsometry can be used to obtain the temperature dependence of two principal components of the dielectric tensor of an orthorhombic layer crystal, as well as the interband critical-point parameters and their temperature dependence.

Measurements have been carried out only on the cleavage planes of GeS. Some differences in the critical-point energies, Lorentzian broadening parameters, and the strengths of the structure as a function of temperature have been obtained for the two polarizations ($\mathscr{E}$ parallel to either **a** or **b** axes), especially at low temperature. In general, no significant change of the excitonic parameter and the oscillator strength of the transitions was observed with increasing temperature for the structure with polarization $\mathscr{E}\|\|\mathbf{b}$, although these parameters exhibited some change for the other polarization direction. The temperature dependence of the CP energies (broadenings) is shown to be similar to that found for the group-IV elemental and III-V compound semiconductors. Fits to these dependences with theoretical expressions yield average phonon frequencies which are reasonable in view of the lattice-vibrational frequencies of the material.

ACKNOWLEDGMENTS

We would like to thank E. Schönherr for the growth of the GeS crystals, G. Kisela and the crystal preparation group at the Max-Planck-Institut für Festkörperforschung for the sample preparation and orientation, and W. Neu for help with the construction of the cryostat. We would also like to thank H. Hirt, M. Siemers, and P. Wurster for expert technical help.

*Permanent address: Solid State Physics Section, First Laboratory, Aristotle University of Thessaloniki, Thessaloniki, Greece.

[1]S. Logothetidis, L. Viña, and M. Cardona, Phys. Rev. B **31**, 2180 (1985).

[2]L. Viña, S. Logothetidis, and M. Cardona, Phys. Rev. B **30**, 1979 (1984).

[3]S. Logothetidis, L. Viña, and M. Cardona, Phys. Rev. B **31**, 947 (1984); L. Viña, H. Höchst, and M. Cardona, *ibid.* **31**, 958 (1985).

[4]R. N. Tauber, A. A. Machonis, and I. B. Cadoff, J. Appl. Phys. **37**, 4855 (1966).

[5]Y. M. Tsang and M. L. Cohen, Phys. Rev. B **3**, 1254 (1971).

[6]E. Schönherr and W. Stetter, J. Cryst. Growth **30**, 96 (1975).

[7]F. Lukeš, E. Schmidt, J. Humlíček, and D. Dub, Phys. Status Solidi B **122**, 679 (1984).

[8]M. Cardona and H. S. Sommers, Jr., Phys. Rev. **122**, 1382 (1961).

[9]R. M. A. Azzam and N. M. Bashara, *Ellipsometry and Polarized Light* (North-Holland, Amsterdam, 1977), Chap. 4.

[10]D. E. Aspnes, J. Opt. Soc. Am. **70**, 1275 (1980).

[11]D. E. Aspnes, J. C. Phillips, K. L. Tai, and P. M. Bridenbaugh, Phys. Rev. B **23**, 816 (1981).

[12]M. Cardona and D. L. Greenaway, Phys. Rev. **133**, A1685 (1964).

[13]M. Cardona, *Modulation Spectroscopy,* Suppl. 11 of *Solid State Physics* (Academic, New York, 1969).

[14]Y. Toyozawa, M. Inoue, T. Inui, M. Okazaki, and E. Hanamura, J. Phys. Soc. Jpn. Suppl. **21**, 133 (1966).

[15]Y. P. Varshni, Physica (Utrecht) **34**, 149 (1967).

[16]C. K. Kim (private communication).

[17]F. Lukeš, E. Schmidt, and A. Lacina, Solid State Commun. **39**, 921 (1981).

[18]P. Lautenschlager, P. B. Allen, and M. Cardona, Phys. Rev. B **31**, 2163 (1985).

[19]H. R. Chandrasekhar, R. G. Humphreys, U. Zwick, and M.

Cardona, Phys. Rev. B **15**, 2177 (1977).
[20]G. E. Jellison, Jr. and F. A. Modine, Phys. Rev. B **27**, 7466 (1983).
[21]T. Grandke, M. Cardona, and L. Ley, Solid State Commun. **32**, 353 (1979).
[22]M. Cardona and G. Harbeke, Phys. Rev. Lett. **8**, 512 (1962).
[23]J. D. Wiley, A. Breitschwerdt, and E. Schönherr, Solid State Commun. **17**, 355 (1975).
[24]J. D. Wiley, D. Thomas, E. Schönherr, and A. Breitschwerdt, J. Phys. Chem. Solids **41**, 801 (1980).